Hypoxia Induces Peroxisome Proliferator–Activated Receptor α (PPARα) and Lipid Metabolism Peroxisomal Enzymes in Human Glioblastoma Cells

G. Laurenti,[1] E. Benedetti,[1] B. D'Angelo,[1] L. Cristiano,[1] B. Cinque,[2] S. Raysi,[3] M. Alecci,[2] M.P. Cerù,[1] M.G. Cifone,[2] R. Galzio,[2] A. Giordano,[4,5**] and A. Cimini[1,4*]

[1]*Department of Basic and Applied Biology, University of L'Aquila, Italy*

[2]*Department of Health Sciences, University of L'Aquila, Italy*

[3]*Neurosurgery Unit, San Salvatore Hospital, L'Aquila, Italy*

[4]*Sbarro Institute for Cancer Research and Molecular Medicine, Temple University, Philadelphia, Pennsylvania*

[5]*Department of Human Pathology and Oncology, University of Siena, Italy*

ABSTRACT

Glioblastoma multiforme (GBM) represents the most severe type of glioma, the most common brain tumor. Their malignancy shows a relationship with an increased proliferation and a poorly organized tumor vascularization, an event that leads to inadequate blood supply, hypoxic areas and at last to the formation of necrotic areas, a feature of glioblastoma. Hypoxic/necrotic tumors are more resistant to chemotherapy and radiation therapies, thus it is crucial to formulate new therapeutic approaches that can render these tumors more sensitive to the action of conventional therapies. It has been demonstrated that under hypoxia, gliomas accumulate lipid droplets and that this event is positively correlated with the degree of malignancy, glioblastoma being the most endowed with lipid droplets. We have previously demonstrated in ex vivo glioma specimens a grade-dependent lipid metabolism perturbation. Here we studied the lipid pathways and the presence of stemness markers in glioma primary cultures, obtained from surgical specimens of patients affected by glioma at different grade of malignancy, GBM primary cultures cultured under both hypoxic and normoxic conditions, as well as normal human astrocytes. The results obtained demonstrate that hypoxia plays a crucial role in regulating the expression of lipid metabolism peroxisomal enzymes, the lipid droplets accumulation as well as the transcription factor PPARα. J. Cell. Biochem. 112: 3891–3901, 2011. © 2011 Wiley Periodicals, Inc.

Glioblastoma multiforme (GBM) represents the most severe type of glioma, the most common brain tumor. This destructive cancer can occur de novo (primary GBM) or as a result of the malignant evolution of a low grade glioma (secondary GBM). However, both tumors, despite being treated with combined radiotherapy and chemotherapy, are characterized by poor prognosis (6–12 months) (Kleihues et al., 2002). As suggested by its name, this tumor is extremely heterogeneous and characterized by a diffuse tissue-distribution pattern, with extensive dissemination of the tumor cells within the brain, an event that thwarts complete surgical resection. Therefore, disease recurrence occurs in the majority of the patients. Their enhanced malignancy shows a relationship with an increased proliferation and a poorly organized tumor vascularization, an event that leads to inadequate blood supply, hypoxic areas and at last to the formation of necrotic areas, a

feature of glioblastoma. Hypoxic/necrotic tumors are more resistant to chemotherapy and radiation therapies, thus it is crucial to formulate new therapeutic approaches that can render these tumors more sensitive to the action of conventional therapies (Amberger-Murphy, 2009). It is known that under hypoxia ATP production is mainly due to glycolytic pathway and not to mitochondrial oxidative phosphorylation. The glycolytic production of ATP is one of the most important characteristics of several tumor cells, also under aerobic conditions, a phenomenon known as the "Warburg effect" (Gatenby and Gillies, 2004; Denko, 2008; La Schiazza et al., 2008). It has been demonstrated that under hypoxia, gliomas accumulate lipid droplets and that this event is positively correlated with the degree of malignancy, glioblastoma being the most endowed with lipid droplets (Opstad et al., 2008). The mechanisms linking cellular replication to lipid metabolism are being studied by

several groups. Some authors have focused on the role of protein prenylation, others on the peroxisome proliferator-activated receptors (PPARs), which are transcriptional factors that regulate the expression of several enzymes involved in lipid metabolism (Lemberger et al., 1996; Van den Heuvel, 1999; Benedetti et al., 2010). Peroxisomes, like mitochondria, consume molecular oxygen and metabolize fatty acids, leaving two carbon atoms per cycle to generate acetyl-CoA in a process called β-oxidation. We have previously demonstrated the presence of lipid droplets in neural stem cells, which disappeared when cells underwent to astroglial differentiation (Cimini et al., 2007). Since GBM cell are enriched of lipid droplets, thus suggesting they may be considered a marker of the undifferentiated status, to study the presence of lipid droplets and lipid metabolism in brain tumor cells may be useful to understand tumor biology.

Understanding the pathways involved in lipid metabolism impairment, probably related to the anaerobic conditions in GBM cells, will allow to get more insight in the biology of this tumor.

The aim of this work was to investigate the roles played by hypoxia on the lipid metabolism and in the acquisition of a "stem" phenotype, in order to find novel approaches able to counteract tumor resistance and recurrences.

In particular, we studied the lipid pathways in glioma primary cultures, obtained from surgical specimens of patients affected by glioma at different grade of malignancy, GBM primary cultures cultured under both hypoxic and normoxic conditions, as well as normal human astrocytes. On these samples, peroxisomal number, peroxisomal enzymes, PPARα and stem markers such as nestin, marker of undifferentiated neuroepithelial cells, and stem cell-derived neural stem/progenitor cell supporting factor (SDNSF) (Toda et al., 2003) have been studied. The results obtained, in a near future, may give the opportunity to design more efficient therapeutic protocols to treat this extremely malignant tumor.

MATERIALS AND METHODS

MATERIALS

Triton X-100, dimethylsulfoxide (DMSO), sodium dodeciylsulfate (SDS), Tween 20, bovine serum albumin (BSA), HOECHST, Nonidet P40, sodium deoxycolate, ethylene diamine tetraacetate (EDTA), phenylmethanesulphonylfluoride (PMSF), sodium fluoride, sodium pyrophosphate, ortovanadate, leupeptin, aprotinin, pepstatin, NaCl, polyvinylidene difluoride (PVDF) sheets, anti-PMP70, anti-SDNSF, glycerol, acetone, fluorescein-labeled anti-rabbit and anti-mouse IgG antibodies, Triacylglycerol (1,2 dimyrystoil-3 palmytoil-rac-glycerol) (TAG), trimyrystin (TRIM), tripalmytoil (TRIP), cholesterol (C) were all purchased from Sigma Chemical CO (St. Louis, CO). Micro-BCA kit was purchased Pierce Biotechnology (Rockford, IL). Anti-AOX was purchased Chemicon (Nuernberg, Germany), anti PPARα was from Affinity Bioreagents Inc. (Golden, CO), Anti THL was a generous gift from Prof. P.P. van Veldhoven KU Leuven Belgium. Anti-PEX14 was a generous gift from Prof. Herdman, University of Bochu, Germany. Horseradish peroxidase (HRP)-conjugated anti-mouse or anti-rabbit IgG secondary antibodies were from S. Cruz Biotechnology (Santa Cruz, CA). Enhanced chemiluminescence (ECL) Bio-Rad Laboratories, (Hercules, CA). Trizol

reagent was purchased from Invitrogen (Paisley, UK). High-Capacity cDNA Reverse Trascription Kit, TaqMan universal PCR master mix and Assay on Demand™ gene expression reagents for human ACOX1, HMGCoA-Red, PEX-14, THIO, PPARα, TATA Box Binding Protein (TBP) were all purchased from Applied Biosystems (Foster City, CA). Vectastain Elite kit, 3,3′- diaminobenzidine DAB Substrate kit for Peroxidase (POD), were purchased from Vector (Burlingame, CA). Eukitt was purchased from Kindler GmbH & Co.(Freiburg, Germany). All other chemicals were of the highest analytical grade.

METHODS

Patient population. The study was approved by the Hospital Ethics Committee, and all patients signed an informed consent before participating in the study. Between April 2008 and December 2009, 100 patients underwent surgical resection for a newly diagnosed primary supratentorial brain glioma at the Department of Neurosurgery, S.Salvatore Hospital, L'Aquila, Italy. Of these patients, 60 were diagnosed according to the World Health Organization (WHO) Grade IV glioma (glioblastoma), 30 with WHO Grade III glioma (astrocytoma), 10 with Grade II glioma (Low grade astrocytoma). Ages ranged from 43 to 73 years, with a mean age of 60 years. All patients underwent a complete clinical and neurological evaluation at the admission in order to evaluate clinical conditions and Karnofsky Performance Status. Before the surgical procedure, a complete neuro-radiological study, including TAC scan without contrast enhancement (c.e.), MRI with and without gadolinium, Technetium 99 MIBI brain APECT, was performed for all patients; in cases of tumor seated near motor and/or speech areas functional MRI (f-MRI) was performed. For this study we selected patients whose lesions were suitable for gross total removal. The surgical technique used foresees tumor aggression from the borders avoiding initial lesion debulking. Surgical removal starts from the edematous brain surrounding the tumor. When possible, the resection includes apparently normal brain tissue and in some selected cases, as in cases of tumors involving brain lobes, especially in non-dominant sites, lobotomy was performed. In all cases, surgical intervention with the aid of Image Guided Surgery was performed and in selected cases of suspected grade IV astrocytoma, 5-aminolevulinic acid, was orally administered before surgical procedures in order to control the extent of tumor resection by Photo Dynamic Diagnosis (PDD). Complete post-operative neuro-radiological investigation was performed in all patients, including TAC scan with and without c.e. within 48 h from surgery and MRI with and without gadolinium performed immediately before and at the end of radiotherapy and each following three months, in association with Technetium 99 MIBI brain SPECT.

Cell cultures. Human Astrocytes were seeded at density of 5,000 cells/cm^2 in poly-L-lysine coated flask with astrocyte complete medium (AM). The culture medium was changed every 3 days until 90% of confluence. The subculture was assessed by using trypsin/EDTA solution, enzymatic digestion was neutralized added complete medium and the cells were replaced at density of 5,000 cells/cm^2 in a new poly-D-lysine coated flask.

Glioma patients who underwent a resection of their tumor in the Neurosurgery Department were included in the study. Individual

tumor biopsies excluding necrotic fragments were maintained in culture medium and addressed to our laboratory. The fragment was rinsed with Hank's balanced salt solution (HBSS), the necrotic areas and red endothelial parts were moved aside. The remaining fragments were finely minced into $0.5\,mm^3$ section pieces approximately. The suspension was centrifuged twice at $1,000g$ for 5 min in HBSS and the supernatant discarded. The enzymatic digestion was carried out by incubating the pellet with 4 ml 0.125% Trypsyn and 0.125% EDTA at 37°C for 10 min. Growth culture medium containing 20% FBS was added to stop the enzymatic digestion. After centrifugation (5 min, $1,000g$), the pellets were resuspended in culture growth medium, and then were transferred to $75\,cm^2$ flask precoated with $2\,\mu g/cm^2$ poly-D-lysine and maintained at 37°C in 5% CO_2, 95% air atmosphere. The cells were cultured in DMEM supplemented with 20% FBS, 2 mM L-glutammine, 50 UI/ml pennycillin–streptomycin until confluence. The culture medium was changed every 2 days. The subculture was assessed by using trypsin (0.05%)/EDTA (0.02%), for 10 min at 37°C. Enzymatic digestion was neutralized by adding an equal volume of culture medium and cells were resuspended and transferred to new flask. The subculture cells were cultured in DMEM supplemented with 10% FBS, 2 mM L-glutammine, 50 UI/ml pennycillin–streptomycin until confluence. The culture medium was changed every 2 days.

Hypoxia induction procedures. Only GBM cells were submitted to hypoxia condition. Hypoxic stress was exerted by placing culture dishes in an airtight chamber. The chamber was sealed and the air was reduced to 0.5 atm by aspiration and replaced by flushing for 30 min with a gas mixture of 95% N_2 and 5% CO_2. The resultant atmosphere contained low oxygen concentration as monitored by the anaerobic indicator BR55. To maintain the temperature at 37°C the chamber was returned to the incubator. The relative humidity was maintained close to 100% by filling the bottom of the chamber with deionized sterile water. Hypoxic shock was applied for 96 h. (Di Loreto et al., 2000).

Treatments. Grade IV primary glioma cell cultures were treated with Temozolomide (stock solution 128 mM in DMSO, c.f. 1 mM) both in normoxic and hypoxic conditions. The PPARα antagonist GW6471 (stock solution 20 mM in DMSO) was used alone at the final concentration of $4\,\mu M$ in normoxia and hypoxia conditions. The combination of Temozolomide (c.f. 1 mM) and GW6471 (cf. $2\,\mu M$) was used for the normoxic cell cultures. In hypoxic cultures the combination was Temozolomide (c.f. 1 mM) and GW6471 (c.f.4 μM). The cells were treated before the hypoxic shock. Hypoxic condition was applied for 24 h.

Protein assay. Proteins were assayed by the micro-BCA kit. Briefly, this assay is a detergent-compatible formulation based on bicinchoninic acid (BCA) for the colorimetric detection and quantitation of total protein. The method combines the reduction of Cu^{2+} to Cu^{1+} by protein in alkaline medium (the biuret reaction) with the high sensitive and selective colorimetric detection of the cuprous cation, using a reagent containing BCA (Smith et al., 1985). The purple-colored reaction product of this assay is formed by the chelation of two molecules of BCA with one cuprous ion. This complex exhibits a strong absorbance at 562 nm.

Western blotting. For Western blotting, cell lysates in ice-cold RIPA buffer (phosphate buffer saline pH 7.4 containing 0.5% sodium deoxycolate, 1% Nonidet P-40, 0,1% SDS, 5 mM EDTA, 100 mM sodium fluoride, 2 mM sodium pyrophosphate, 1 mM PMSF, 2 mM ortovanadate, $10\,\mu g/ml$ leupeptin, $10\,\mu g/ml$ aprotinin, $10\,\mu g/ml$ pepstatin) were centrifuged and the supernatants were assayed for protein content. Twenty to thirty micrograms of proteins were electrophoresed through a 7.5–15% SDS polyacrilamide gel under reducing condition. Proteins were transferred onto PVDF membrane sheets and nonspecific binding sites were blocked for 1 h at room temperature (RT) in 20 mM TRIS–HCl buffer, 55 mM NaCl, and 0.1% Tween 20 pH 7.4 (TBST) containing 5% non-fat dry milk (blocking solution). Membranes were then incubated overnight at 4°C with rabbit anti-THL (1:1,000), anti-PMP70 (1:3,000), anti-GFAP (1:1,000), anti-PPARα (1:100) antibodies, and mouse anti-ß tubulin III (1:1,000), all dissolved in blocking solution. After extensive washings with TBST, membranes were incubated with HRP-conjugated anti-mouse or anti-rabbit IgG secondary antibody (1:2,000). Immunoreactive bands were visualized by ECL, according to the manufacturer's instructions. Band relative densities were determined using TotalLab software (ABEL Science-Ware srl, Italy) and values were given as relative units (RU). Immunoblot data were normalized to total protein load by quantification of all samples in a single assay before loading, and confirmation of equal loading by image analysis and scanned Coomassie blue-stained gels after blotting (Benedetti et al., 2010).

Real time PCR. Total mRNA was harvested with the Trizol reagent according to the manufacturer's protocol. The gene expressions were quantified in a two-step reverse transcription-polymerase chain reaction (RT-PCR). Complimentary DNA was reverse transcribed from total RNA samples using High-Capacity cDNA reverse Trancription Kit. PCR products were synthesized from cDNA using the TaqMan universal PCR master mix and Assays on Demand gene expression reagents for human ACOX1, HMGCoA-Red, THIO, PPARα (Assay ID: Hs 00244515_m1, Hs00168352_m1, Hs00190073_m1, Hs00155616_m1, Hs00231882_m1). Measurements were made using the ABI Prism 7300HT sequence detection system, according to the manufacturer's protocol. As an endogenous control for these PCR quantification studies, TBP gene expression assay was used. Results represent normalized ACOX1, THIO, HMGCoA-Red, PPARα mRNA amounts relative to healthy tissue using the $2^{-\Delta\Delta Ct}$ method (Livak and Schmittgen, 2001). Each experiment was repeated in triplicate.

Immunofluorescence. Cells growth on poly-L-lysine coated cover lips, after 96 h of hypoxia or normoxia were washed twice with PBS, fixed for 10 min at RT in 4% paraformaldehyde in PBS and permeabilized in PBS containing 0.1% Triton X-100 for 10 min at RT. Nonspecific binding sites were blocked for 30 min with 3% BSA in PBS. Cells were then incubated with mouse anti GFAP (1:400), anti SDSNF (1:200), rabbit anti Nestina (1:100), anti β-tubulin III (1:500), anti PPARα (1:100), anti PMP70 (1:250), anti PEX14 (1:500), anti hypoxia induced factor 1-α (HIF-1α) (1:100) in PBS containing 3% BSA overnight at 4°C. After extensive washings with PBS the cells were incubated with AlexaFluor 488 (rabbit or mouse) secondary antibody (1:2,000 in PBS containing 3% BSA) 30 min at RT. After extensive washings with PBS, cells were mounted with Vectashield mounting medium and photographed at fluorescence microscope AXIOPHOT, Zeiss, microscope.

Bodipy staining. Cells grown on cover lips after 96 h of hypoxia or normoxia were washed twice with PBS, fixed for 10 min at RT in 4% paraformaldehyde in PBS and permeabilized in PBS containing 0.1% Triton X-100 for 10 min at RT. A stock solution of BODIPY 493/503 1 mg/ml in ethanol was prepared and then stored at −20 in the dark until required. Before use, BODIPY stock solution was diluted 1:1,000 in PBS and used for incubate cover lips in the dark for 10 min. After incubation the cells were washed with PBS, mounted with Vectashield mounting medium and photographed at fluorescence microscope AXIOPHOT, Zeiss microscope.

Image analysis. Cells were viewed with a Zeiss Axiophot epifluorescence microscope equipped with a digital camera interfaced with a PC. Images were processed using free software ImageJ 1.44o (Rasband, W.S., ImageJ, U.S. National Institutes of Health, Bethesda, Maryland, http://imagej.nih.gov/ij/, 1997–2011). To quantify the lipid droplets content, the acquired images were taken with 8-bits levels and the average background noise, calculated from four ROI external to the cells was subtracted from the images. The average signal level measured in the cell nucleus was taken as reference and subtracted to the whole image to obtain a reference mask. This was used first to measure the cytoplasm area and then, after a three times the nuclear signal threshold, the residual lipid droplets area. The ratio between these two areas was used to compare cells in the normoxic and hypoxic conditions.

Proliferation assay. Proliferation in control and treated cells was studied by following the incorporation of 5-bromo-2′-deoxy-uridine into cellular DNA (5-Bromo-2′-deoxy-uridine Labeling and Detection Kit III, Roche). The amount of BrdU incorporated is determined by a standard ELISA protocol, which involves "tagging" the incorporated nucleotide with an anti-BrdU antibody. Cells cultured in a 96-well microplate are incubated with BrdU. The labeled cells are fixed with ethanol. Prior to incubation with a monoclonal antibody to BrdU, DNA is partially digested with nucleases to allow the antibody to access BrdU. Next, the anti-BrdU antibody, labeled with POD, is added. Finally, the POD substrate ABTS is added. POD catalyzes the cleavage of ABTS, producing a colored reaction product. The absorbance of the samples 405 nm is determined with a spectrophotometric microplate reader (Infinite F200 Tecan).

Apoptosis measurements. Determination of cytoplasmic histone-associated DNA fragments was performed by using the Cell Death Detection ELISA Kit, following the instructions of the manufacturer. Briefly the assay is based on the quantitative sandwich-enzyme-immunoassay-principle using mouse monoclonal antibodies direct against DNA and histones, respectively. The absorbance peak at 405 nm was measured in a spectrophotometric microplate reader. The results are expressed as absorbance measurement, resulting from the activity of peroxidise conjugated anti-DNA antibody complexed with mono- and oligo-nucleosomes released into the cytoplasm of treated cells, compared with the control.

Lipid extraction. Cell pellets were dissolved in a buffer containing Tris-HCl 20 mM pH 7.4, 1 μM PMSF, 10 μM leupeptin, 10 μM pepstatin, 1 μM aprotinin. After the incubation time (5 min at 4°C), samples were sonicated (5 W, 80% output, 1 min and 50 sec, alternating 10 sec sonication and 10 sec pause) with a Vibracell

sonicator (Sonic and Materials Inc., Danbury, CT). Protein concentration of cell lysates was determined trough the BioRad Protein Assay (Hercules, CA), with BSA standards. Lipids were extracted by the sequential addition of 400 μl methanol, 500 μl chloroform, and 200 μl water. Samples were stirred for 2 min on a vortex-mixer and centrifuged at 10,800g for 10 min. The extraction and centrifugation steps were repeated twice. The organic phases, obtained from different extraction steps were collected, dried under nitrogen, and then analyzed by TLC.

Thin layer chromatography. TLC was performed on 20 cm × 20 cm aluminum silica plates. Eluent mixture (hexane/diethyl ether/acetic acid, 70:30:1) (80:20:2 v/v) (100 ml) was introduced into an eluition tank to separate neutral lipids. Lipids were applied on silica plates as thin rows at 2 cm distance above the bottom of the silica plate, air dried and placed immediately in the eluition tank. The solvent was allowed to ascend to 1 cm from the top of the plate, and then the plate was removed, air-dried and stained. Triacylglycerol (1,2 dimyrystoil-3 palmytoil-rac-glycerol), TRIM, tripalmytoil (TRI), cholesterol (C), cholesteryl-ester (CE), were used as standards. TLC staining was obtained by vaporizing 10% phosphomolybdic acid solution on plates. Phosphomolybdic acid solution was prepared by dissolving 10 g in 100 ml ethanol. The plates were dried for 10 min at 80°C.

STATISTICAL ANALYSIS

For statistical analysis samples were processed by SPSS software and analyzed by ANOVA test, followed by Scheffe's post hoc test" analysis. $^*P < 0.05$, $^{**}P < 0.005$, $^{**}P < 0.0005$. All data are mean ± SD of five separate experiments.

RESULTS

The glioma primary cell cultures, at different grade of malignancy, have been first characterized for the expression of GFAP, in order to identify their astrocytic origin, β-tubulin III, marker of glioma malignancy (Katsetos et al., 2009), and markers of the undifferentiated status such as nestin and SDNSF and compared with normal human astrocytes (Fig. 1). GFAP is present, other than normal astrocytes, also in glioma cultures, unrespect to the grade of malignancy, thus confirming the astrocytic origin of the tumor. β-tubulin III is absent in normal astrocytes while it increase with the grade of malignancy. The same picture appears for nestin and SDNSF, where the higher expression is observed in glioblastoma cultures with the normal astrocytes completely negative.

Since we have previously demonstrated an up-regulation of peroxisomes and peroxisomal related proteins as function of malignancy grade in human glioma (Benedetti et al., 2010), the cultures were then characterized for the presence of peroxisomes by the immunolocalization of the peroxisomal membrane proteins PMP70 and for the presence of lipid droplets (Fig. 2). It clearly appears the increase with the grade of malignancy, of peroxisomes immunopositive cells as well as of the lipid droplets number.

Once confirmed the data previously observed ex vivo on surgical specimens, the attention was focalized on the glioblastoma cultures
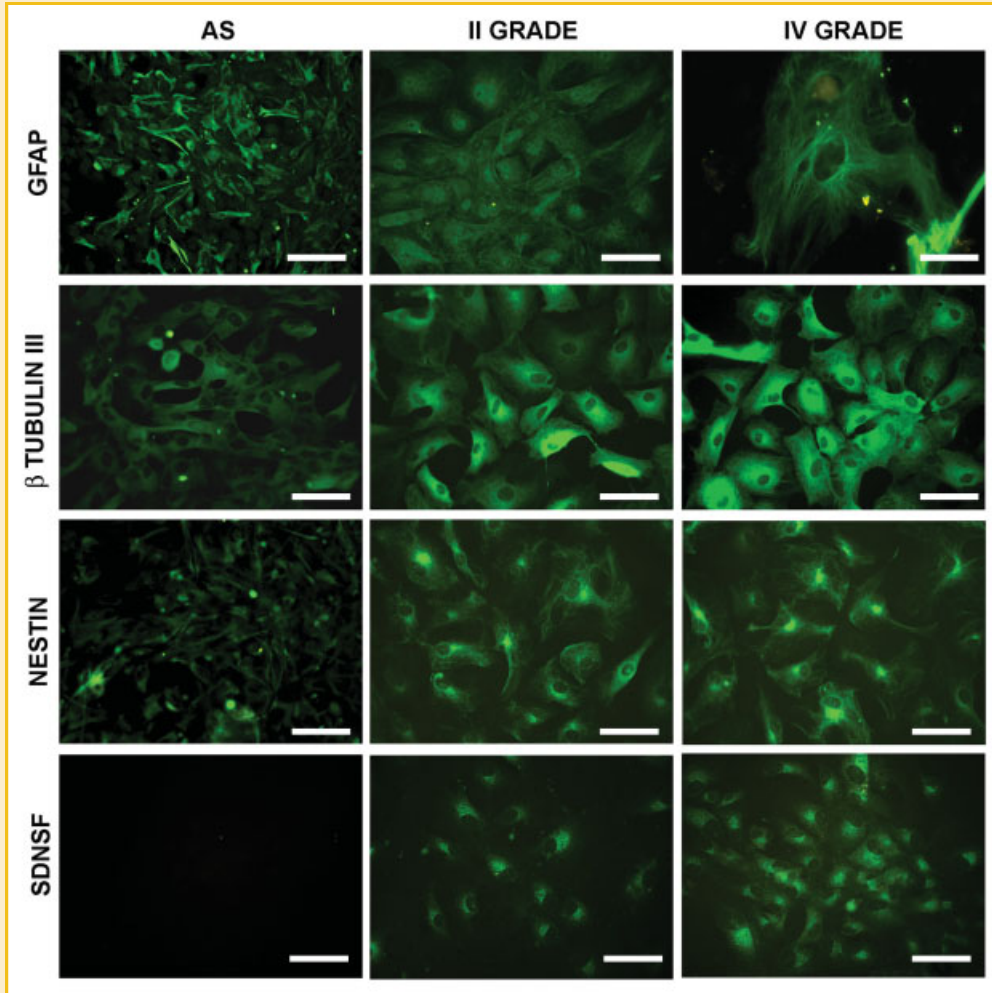
Fig. 1. Immunolocalization of GFAP, β–tubulin III, nestin and stem cell–derived neural stem/progenitor cell supporting factor (SDNSF) in normal human astrocytes and in low and high grade gliomas. Bar = 60 μm. [Color figure can be seen in the online version of this article, available at http://wileyonlinelibrary.com/journal/jcb]
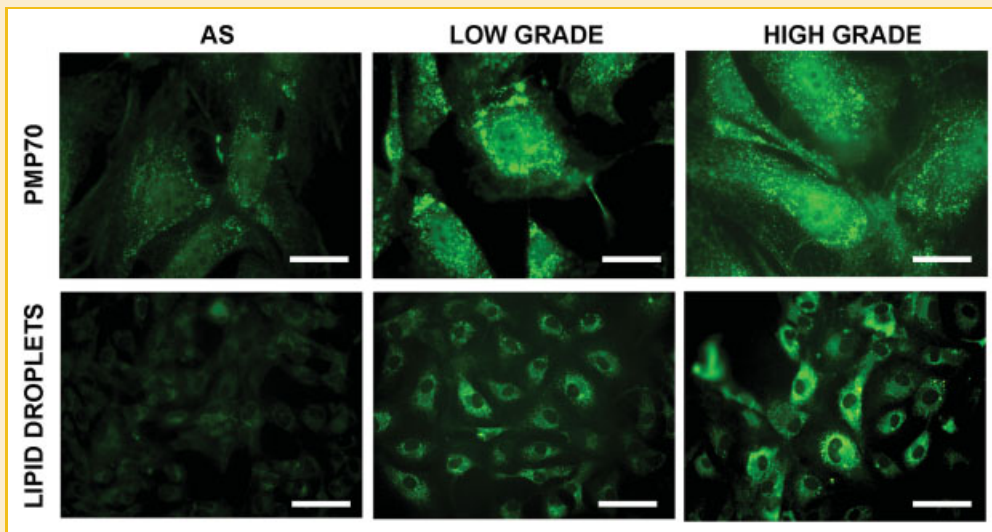

Fig. 2. Immunolocalization of the peroxisomal membrane protein PMP70 and localization of lipid droplets by Bodipy staining in normal human astrocytes and in low and high grade gliomas. Bar = 15 μm and 60 μm, respectively. [Color figure can be seen in the online version of this article, available at http://wileyonlinelibrary.com/journal/jcb]
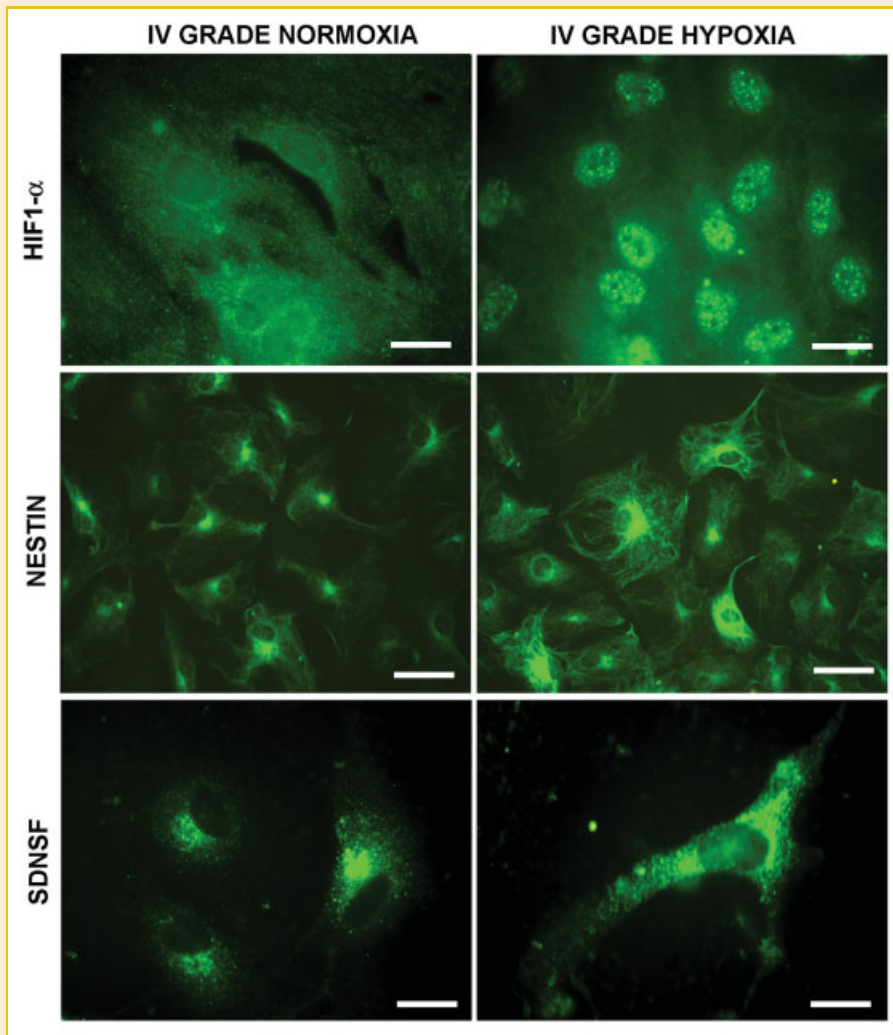
Fig. 3. Hypoxia factor 1α, nestin, and SDNSF localization in glioblastoma cells under normoxic and hypoxic conditions. Bar = 15 μm, 60 μm, and 15 μm, respectively. [Color figure can be seen in the online version of this article, available at http://wileyonlinelibrary.com/journal/jcb]

cultured under normoxic and hypoxic conditions, since the particular hypoxic environment of high grade gliomas.

The first parameter investigated was the HIF1-α localization (Fig. 3). The immunolocalization of HIF1-α shows that in GBM cells in normoxic condition the transcription factor is localized at cytoplasmatic level. Upon hypoxia HIF1-α is upregulated and completely localized to the nuclei, thus suggesting its activation. In the same figure, the localization of stemness markers, such as nestin and SDNSF under normoxia and hypoxia is also shown.

The GFAP astrocytic marker, the malignancy marker β–tubulin III were then investigated under hypoxia (Fig. 4). It appears that hypoxia completely downregulates GFAP while increasing β-tubulin III, thus suggesting its involvement in the acquisition of a more undifferentiated phenotype.

Under hypoxia peroxisomal number, evaluated by PMP70, appears upregulated (Fig. 5) as well as the peroxisomal enzymes involved in the peroxisomal β-oxidation of fatty acids such as acyl-CoA oxidase (AOX) and thiolase (Fig. 6), thus indicating an upregulation of the peroxisomal enzymes and an increase of anti-oxidant defenses. The rate limiting enzyme of mevalonate (MVA) pathway appears upregulated in GBM unrespective to the culture conditions (Fig. 6). The transcription factor PPARα, responsible for the transcription of AOX, thiolase, and catalase genes, is strongly increased and mainly localized to the nuclei, thus suggesting its activation (Fig. 5).

Also lipid droplets are strongly upregulated by hypoxia (Fig. 7), as demonstrated by the quantitative imaging analysis. Moreover they appear also directionally disposed. This is further confirmed by TLC analysis (Fig. 7), where an increase of cholesterol, cholesterol esters, and triglycerides is observed under hypoxia both in low and high grade gliomas, particularly in high grade glioma cells. Interestingly, in hypoxia conditions and only in high grade gliomas, a band corresponding to a diacylglerol is observed.
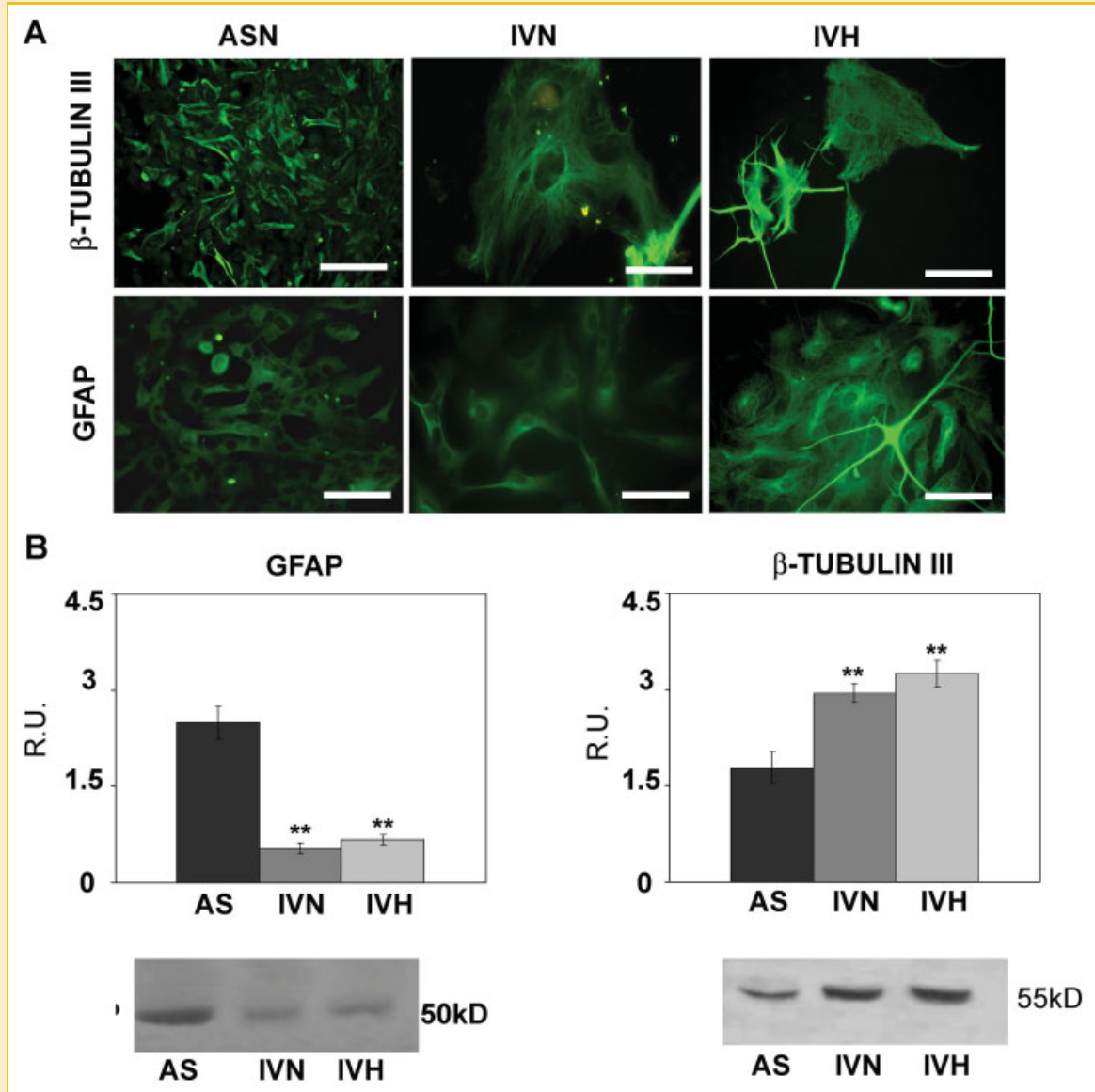
Fig. 4. GFAP and ß–tubulin III immunolocalization and western blotting analysis. Bar = 60 μm. Data are mean of five experiments ± SD. **, *P* < 0.005. [Color figure can be seen in the online version of this article, available at http://wileyonlinelibrary.com/journal/jcb]

DISCUSSION

The prognosis and biological behavior of malignant gliomas are closely related to the different molecular backgrounds of each type of glioma (Kleihues and Cavanee, 2000). Furthermore, the ability of several low-grade gliomas to progress into more aggressive tumors has allowed cancer researchers to elucidate several pathways implicated in the molecular biology of these devastating tumors. Many cancer cells consume glucose avidly and produce lactic acid rather than catabolizing glucose via the TCA cycle, which is key for generating ATP in nonhypoxic normal cells. The shift toward lactate production in cancer, even in the presence of adequate oxygen, is termed the Warburg effect or aerobic glycolysis. (Warburg, 1958). In addition to oncogenic activation of aerobic glycolysis, the

activation of hypoxia inducible factor (HIF), a transcription factor that is stabilized in response to hypoxia, also significantly contributes to the conversion of glucose to lactate. HIF-1 consists of an oxygen sensitive HIF-1α subunit that heterodimerizes with HIF-1β to bind DNA. In high oxygen tension, HIF-1α is hydroxylated by prolyl hydroxylases (PHD) using α-ketoglutarate derived from the TCA cycle. The hydroxylated HIF-1α subunit is recognized by the von Hippel Lindau (VHL) protein and destined for degradation by proteasomes, such that HIF-1α is continuously synthesized and degraded under nonhypoxic conditions. Hypoxia is a pathophysiologic stimulus of anaerobic glycolysis that through the stabilization of HIF-1α transactivates glycolytic enzyme genes. Hence, adaptation to the hypoxic tumor microenvironment results in increased glucose uptake and lactate production. Several
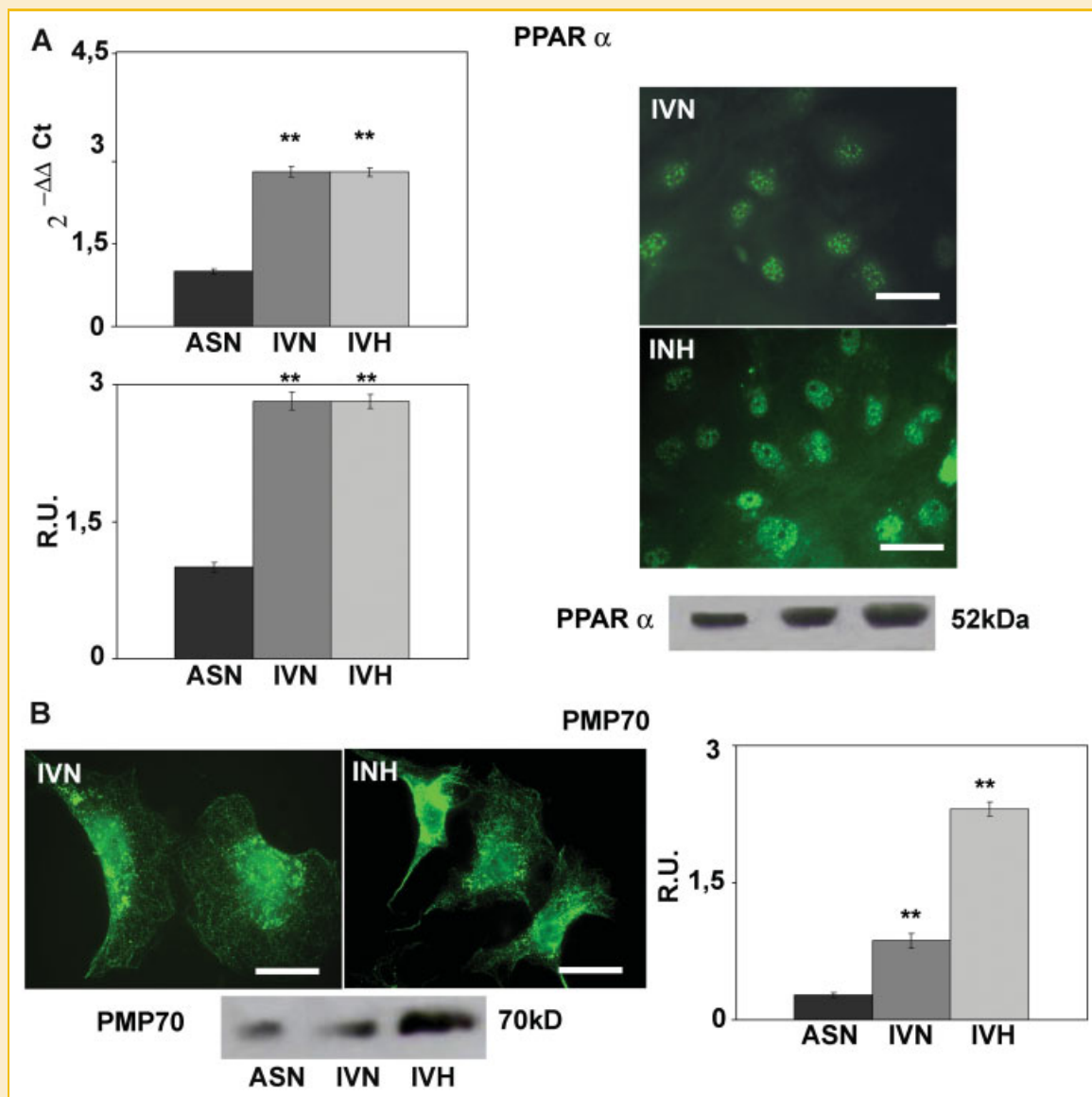
Fig. 5. PPARα immunolocalization, western blotting and Real−time PCR analyses. Bar = 50 μm. Data are mean of five experiments ± SD. **, $P < 0.005$. In the bottom PMP70 immunolocalization and western blotting analysis. Bar = 25 μm. Data are mean of five experiments ± SD. **, $P < 0.005$. [Color figure can be seen in the online version of this article, available at http://wileyonlinelibrary.com/journal/jcb]

oncogenes have been implicated in the Warburg effect. The AKT oncogene mobilizes glucose transporter to the cells surface to enhance glucose uptake and activates hexokinase 2 (HK2) to phosphorylate and trap intracellular glucose. Although not coupled to oxidative phosphorilation, in tumor cells, TCA cycle ensures the efflux of biosynthetic intermediates for lipid and amminocid synthesis, a process called cataplerosis. Citrate is, for instance, transferred from the mithocondrial matrix to the cytosol to be cleaved by ATP citrate lyase (ACL) into oxaloacetate and acetyl-CoA, a lipogenic precursor of giving rise to isoprenoid, cholesterol, and fatty acid. (Feron, 2009). Although the Warburg effect has been recognized since 1920s, less well appreciated are alterations in lipid metabolism and the high rates of de novo fatty acid biosynthesis exhibited by many tumors (Medes et al., 1953). The

cholesterol synthesis is mediated by MVA pathway which uses acetyl-CoA as substrate. Several investigations have shown an abnormally active de novo synthesis of cholesterol from acetate and MVA in malignant glial cells, compared with their normal counterparts (Azarnoff et al., 1958; Goldstein and Brown, 1990). The MVA pathway produces various end products that are critical for functioning in both normal and cancerous cells. These products include cholesterol, dolichol, ubiquinone, isopentenyladenine, geranylgeranyl pyrophosphate, and farnesyl pyrophosphate (Goldstein and Brown, 1990). The rate-limiting step of the MVA pathway is the conversion of 3-hydroxy-3-methylglutaryl CoA (HMG-CoA) to MVA, which is catalyzed by HMG-CoA reductase (Goldstein and Brown, 1990). Blockade of this pathway by HMG-CoA reductase inhibitors results in decreased levels of MVA and
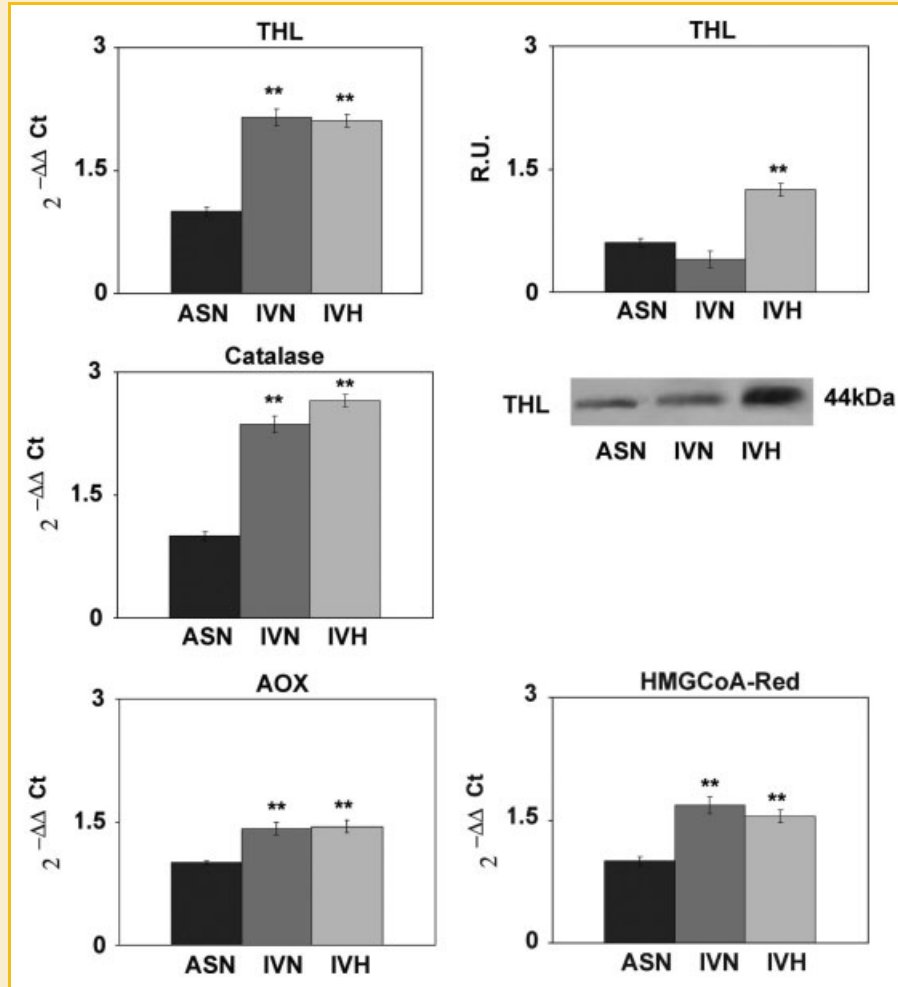
Fig. 6. Left panel: Real–time PCR analysis for the peroxisomal enzymes thiolase, catalase, and Acyl–CoA oxidase (AOX). Data are mean of five experiments ± SD. $^{**}P < 0.005$. In the right panel, western blotting analysis for thiolase and Real–Time PCR analysis for HMGCoA reductase. Data are mean of five experiments ± SD. $^{**}P < 0.005$.

its downstream products and, thus, may have significant influences on many critical cellular functions (Carlberg et al., 1996). Malignant cells seem highly dependent on the sustained availability of the end products of the MVA pathway (Chan et al., 2003). Deregulated or elevated activity of HMG-CoA reductase has been shown in a range of different tumors (Chan et al., 2003). The statin family of drugs, widely used as hypercholesterolemia treatments, is a potent inhibitor of HMG-CoA reductase (Hunninghake, 1992; Corsini et al., 2005).

Recent analyses have shown that statin treatment can directly block tumor cell growth, invasion, and metastatic potential both in vitro and in vivo (Keyomarsi et al., 1991; Agarwal et al., 1999; Bouterfa et al., 2000; Denoyelle et al., 2001; Chan et al., 2003; Wong et al., 2006). The mechanisms linking cellular replication to lipid metabolism have been under study by several groups. Some Authors have focused on the role of protein prenylation (Jackson et al., 1990), others on the PPARs, which are transcriptional factors that regulate the expression of several enzymes involved in lipid metabolism (Feige et al., 2006; Benedetti et al., 2010).

Peroxisomes, like mitochondria, consume molecular oxygen and metabolize fatty acids, cleaving two carbon atoms per cycle to generate acetyl-CoA in a process called β-oxidation. However, peroxisomal β-oxidation is not coupled to ATP synthesis for energy production. The content and function of the enzymes within the peroxisome may vary in the different cell types. In environments with competing metabolic needs, the physiological needs of the cellular environment dictate the state of the peroxisome population and peroxisomal protein content (Keller et al., 1993, 2000). In our previous study we have demonstrated that peroxisomal number and peroxisomal enzymes, mainly those related to lipid metabolism, are strongly upregulated in function of the glioma malignancy grade (Benedetti et al., 2010), in this study we evaluated the expression profiles of several peroxisomal proteins on primary cultures derived from patients affected by glioma at different grades of malignancy. The results obtained confirmed the upregulation of peroxisomes and peroxisomal proteins as function of the malignancy grade. These findings appear conceivable if the strong lipid metabolism perturbation observed in gliomas is considered. In fact, peroxisomes other than catalyze the ß-oxidation pathway with acetyl-CoA
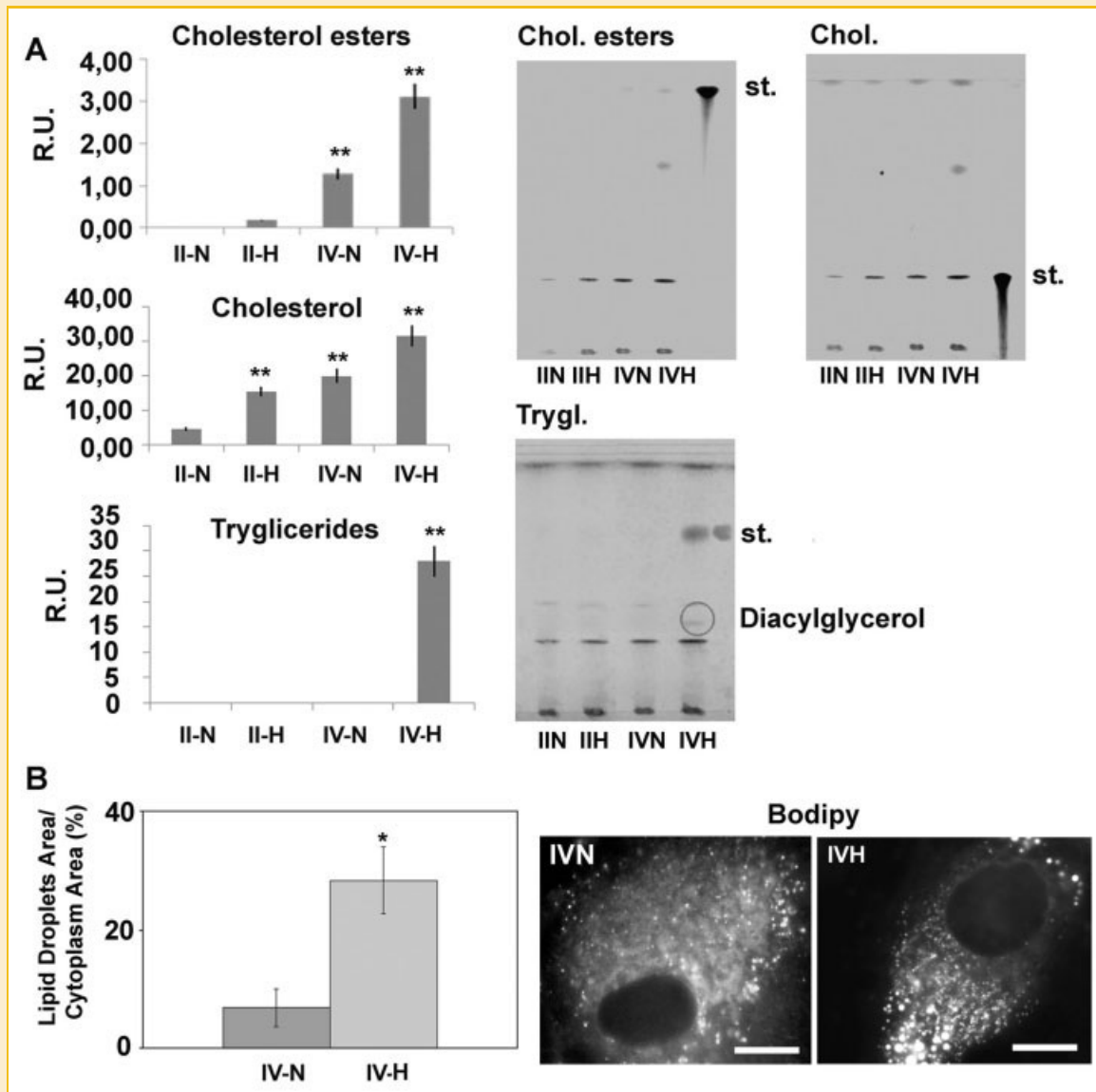
Fig. 7. Panel A: TLC analysis in low grade and high grade gliomas in normoxic and hypoxic conditions. Data are mean of five experiments ± SD. **$P < 0.005$. Panel B: Shows an example of bodipy staining for lipid droplets and the relative quantitative imaging analysis. Bar = 15 μm. Data are mean of four experiments ± SD. *$P < 0.05$.

production, which constitutes the substrate for MVA synthesis, are also involved in MVA pathway, since some enzymes of this pathway such as MVA kinase and MVA diphosphate decarboxylase are localized to peroxisomes and the rate-limiting enzyme, the HMGCoA-Red is localized also to peroxisomes (Kovacs et al., 2007). Finally, peroxisomes are also involved in lipid and dolichol biosynthesis.

The up-regulation of peroxisomes and peroxisomal related proteins, with respect to the control condition, was further stressed by the hypoxia condition to levels comparable to those observed in vivo, thus suggesting that hypoxia and the subsequent metabolic cascade are able to increase peroxisomal number and proteins. This is further supported by the observation, under hypoxia, of the complete nuclear localization of PPARα, suggesting the activation of the nuclear receptor. The activation of PPARα under hypoxic

conditions is also supported by the significant increase of AOX, and thiolase transcripts, that are known to be under PPARα transcriptional control. Moreover, in the in vitro model, as observed in vivo, lipid droplets increase as a function of the malignancy grade and in particular, under hypoxic conditions, as well as the lipid components such as tryglicerides, CEs, and cholesterol, thus confirming the crucial metabolic role of hypoxia and of the hypoxia factor 1α that appears completely localized to the nuclei in this condition.

On the overall, our data indicate that peroxisomes are strongly involved in glioma biology and that their number and enzymatic content appear upregulated as function of malignancy grade. Thus, correlating the malignancy grade with the expression of peroxisomal genes and proteins may constitute a more sensitive tool to be predictive of the progression of the tumor.

Further experiments are in progress in order to investigate the roles of the other PPAR isotypes and also the effects of PPAR antagonists/agonist alone or in combination with the final aim to counteract chemoresistance and recurrences.

ACKNOWLEDGMENTS

REFERENCES

Agarwal B, Bhendwal S, Halmos B, Moss SF, Ramey WG, Holt PR. 1999. Lovastatin augments apoptosis induced by chemotherapeuticagents in colon cancer cells. Clin Cancer Res 5:2223–2229.

Amberger-Murphy V. 2009. Hypoxia helps glioma to fight therapy. Curr Cancer Drug Targets 9:381–390.

Azarnoff DL, Curran GL, Williamson WP. 1958. Incorporation of acetate-1-C14 into cholesterol by human intracranial tumors in vitro. J Natl Cancer Inst 21:1109–1115.

Benedetti E, Galzio R, Laurenti G, D'Angelo B, Melchiorre E, Cifone MG, Fanelli F, Muzi P, Coletti G, Alecci M, Sotgiu A, Cerù MP, Cimini A. 2010. Lipid metabolism impairment in human gliomas: Expression of peroxisomal proteins in human gliomas at different grades of malignancy. Int J Immunopathol Pharmacol 23:235–246.

Bouterfa HL, Sattelmeyer V, Czub S, Vordermark D, Roosen K, Tonn JC. 2000. Inhibition of Ras farnesylation by lovastatin leads the down-regulation of proliferation and migrating in primary cultured human glioblastoma cells. Anticancer Res 20:2761–2771.

Carlberg M, Dricu A, Blegen H. 1996. Mevalonic acid is limiting or N-linked glycosylation and translocation of the insulin-like growth factor-1 receptor to the cell surface. Evidence for a new link between 3-hydroxy-3-methyl-glutaryl-coenzyme a reductase and cell growth. J Biol Chem 27:17453–17462.

Chan KK, Oza AM, Siu LL. 2003. The statins as anticancer agents. Clin Cancer Res 9:10–19.

Cimini A, Cristiano L, Benedetti E, D'Angelo B, Cerù MP. 2007. PPARs expression in adult mouse neural stem cells: Modulation of PPARs during astroglial differentiaton of NSC. PPAR Res 2007:48242.

Corsini A, Bellosta S, Davidson MH. 2005. Pharmacokinetic interactions between statins and fibrates. Am J Cardiol 96:44K–49K.

Denko NC. 2008. Hypoxia, HIF1 and glucose metabolism in the solid tumour. Nat Rev Cancer 8:705–713.

Denoyelle C, Vasse M, Korner M, Mishal Z, Ganne F, Vannier JP, Soria J, Soria C. 2001. Cerivastatin, an inhibitor of HMG-CoA reductase, inhibits the signaling pathways involved in theinvasiveness and metastatic properties of highly invasive breast cancer cell lines: An *in vitro* study. Carcinogenesis (Lond) 22:1139–1148.

Di Loreto S, Corvetti L, Maccarone R, Piancatelli D, Adorno D. 2000. Interleukin 1-beta modulates the effects of hypoxia in neuronal culture. J Neuroimmunol 106:32–42.

Feige JN, Gelman L, Michalik L, Desvergne B, Wahli W. 2006. From molecular action to physiological outputs: Peroxisome proliferator-activated receptors are nuclear receptors at the crossroads of key cellular functions. Progr Lipid Res 45:120–159.

Feron O. 2009. Pyruvate into lactate and back: From the Warburg effect to symbiotic energy fuel exchange in cancer cells. Radiother Oncol 92:329–333.

Gatenby RA, Gillies RJ. 2004. Why do cancers have high aerobic glycolysis? Nat Rev Cancer. 2004 4:891–899.

Goldstein JL, Brown MS. 1990. Regulation of the mevalonate pathway. Nature 343:425–430.

Hunninghake DB. 1992. HMG-CoA reductase inhibitors. Curr Opin Lipidol 3:22–28.

Jackson JH, Cochrane CG, Bourne JR, Solski PA, Buss JF, Der CJ. 1990. Farnesol modification of kirsten-ras exon 4B protein is essential for transformation. Proc Natl Acad Sci USA 87:3042–3046.

Katsetos CD, Dráberová E, Legido A, Dumontet C, Dráber P. 2009. Tubulin targets in the pathobiology and therapy of glioblastoma multiforme. I. Class III beta-tubulin. J Cell Physiol 221:505–513.

Keller JM, Collet P, Bianchi A. 2000. Implications of peroxisome proliferator-activated receptors (PPARS) in development, cell life status and disease. Int J Dev Biol 44:429–442.

Keller J, Cablè S, El Bouhtoury F, Heusser S, Scotto C, Armbruster L, Ciolek E, Colin S, Schilt J, Dauca M. 1993. Peroxisome trough cell differentiation and neoplasia. Biol Cell 77:77–78.

Keyomarsi K, Sandoval L, Band V, Pardee AB. 1991. Synchronization of tumor and normal cells from G1 to multiple cell cycles by lovastatin. Cancer Res 51:3602–3609.

Kleihues P, Louis DN, Scheithauer B, Rorke LB, Reifenberg G, Burger PC, Webster K, Cavenee WK. 2002. The WHO classification of tumors of the nervous system. J Neuropathol Exp Neurol 61:215–225.

Kleihues P, Cavanee WK. 2000. Pathology and genetics of tumors of the nervous system. Lyon, France: IARC Press.

Kovacs WJ, Tape KN, Shackelford JE, Duan X, Kasumov T, Kelleher JK, Brunengraber H, Krisans SK. 2007. Localization of the pre-squalene segment of the isoprenoid biosynthetic pathway in mammalian peroxisomes. Histochem Cell Biol 127:273–290.

La Schiazza R, Lamari F, Foglietti MJ, Hainque B, Bernard M, Beaudeux JL. 2008. Cellular energetic metabolism of cerebral tissue: Metabolic characteristics of glial tumours. Ann Biol Clin (Paris) 66:131–141.

Lemberger T, Desvergne B, Wahli W. 1996. Peroxisome proliferator-activated receptors: A nuclear receptor signaling pathway in lipid physiology. Annu Rev Cell Dev Biol 12:335–363.

Livak KJ, Schmittgen TD. 2001. Analysis of relative gene expression data using real-time quantitative PCR and the 2(-Delta Dealta C(T)) method. Methods 25:402–408.

Medes G, Thomas A, Weinhouse S. 1953. Metabolism of neoplastic tissue. IV. A study of lipid synthesis in neoplastic tissue slices in vitro. Cancer Res 13:27–29.

Opstad KS, Bell BA, Griffiths JR, Howe FA. 2008. An investigation of human brain tumour lipids by high-resolution magic angle spinning 1H MRS and histological analysis. NMR Biomed 21:677–685.

Smith PK, Krohn RI, Hermanson GT, et al. 1985. Measurement of protein using bicinchoninic acid. Anal Biochem 150:76–85.

Toda H, Tsuji M, Nakano I, Kobuke K, Hayashi T, Kasahara H, Takahashi J, Mizoguchi A, Houtani T, Sugimoto T, Hashimoto N, Palmer TD, Honjo T, Tashiro K. 2003. Stem cell-derived neural stem/progenitor cell supporting factor is an autocrine/paracrine survival factor for adult neural stem/progenitor cells. J Biol Chem 278:35491–35500.

Van den Heuvel JP. 1999. Peroxisome proliferator-activated receptors: A critical link among fatty acids, gene expression and carcinogenesis. J Nutr 129:575S–580S.

Warburg O. 1958. On the origin of cancer cells. Science 123:309–314.

Wong WW, Dimitroulakos J, Minden MD, Penn LZ. 2006. HMG-CoA reductase inhibitors and the malignant cell: The statin family of drugs as triggers of tumor-specific apoptosis. Leukemia 16:508–519.